A dynamical mean-field approximation study of a tight-binding model for $Ga_{1-x}Mn_xAs$

A.-M. Nili,[1] U. Yu,[2] J. Moreno,[1] D. Browne,[1] and M. Jarrell[1]

[1]*Department of Physics and Astronomy & Center for Computation and Technology,*
Louisiana State University, Baton Rouge, Louisiana 70803, USA
[2]*Department of Applied Physics, Gwangju Institute of Science and Technology, Gwangju 500-712, Korea*
(Dated: July 28, 2010)

The magneto-optical properties of the ferromagnetic semiconductor $Ga_{1-x}Mn_xAs$ are studied within the dynamical mean-field approximation (DMFA). A material-specific multiband sp^3 tight-binding Hamiltonian is employed for the dispersion of the GaAs host. The calculated density of states shows an impurity band and a distorted valence band for large and moderate values of magnetic coupling, respectively. Upon using the more realistic band structure, the ferromagnetic transition temperature is significantly closer to the experimental results than the previous predictions of $k \cdot p$ models. The optical conductivity shows a Drude-like peak at low frequencies which is suppressed by increasing of the magnetic coupling.

Introduction- The discovery of a new generation of dilute magnetic semiconductors (DMS) with large Curie temperature[1,2] has led to numerous experimental and theoretical studies.[3,4] The ultimate goal is to find a DMS with a ferromagnetic transition above room temperature and suitable for use in spintronic devices. One of the most promising candidates is $Ga_{1-x}Mn_xAs$ due to its rather high T_c,[1,3] and compatibility with current electronic applications. Despite this interest, some of the most basic questions about $Ga_{1-x}Mn_xAs$ are still unanswered after more than a decade of its discovery. Among them are questions about the nature of its underlying magnetic interactions and the role of the impurity band.

In this work we combine the sp^3 tight-binding Hamiltonian for the zinc blende GaAs with the self consistent dynamical mean-field approximation (DMFA) to study the magnetic and transport properties of $Ga_{1-x}Mn_xAs$. We assume that the manganese (Mn) doping does not alter the tight-binding parameters of GaAs and any change in the band structure is due to the many-body effects induced by the magnetic coupling between the Mn local moments and the itinerant holes.

Several previous studies have used the tight-binding approximation for DMS. Tang and Flatté calculated the local density of states for a single Mn and two nearby Mn impurities[5] and the magnetic circular dichroism[6] of bulk $Ga_{1-x}Mn_xAs$ using large supercells; Mašek *et al.* took the Weiss mean-field approach to calculate the electronic structure for several DMS[7]; and Turek *et al.* compared both tight-binding approaches[8,9]. Large-scale Monte-Carlo studies of real-space tight-binding Hamiltonians including only the three valence bands has also been performed[10].

Our DMFA calculation incorporates quantum self-energy corrections which were not included in most of the studies described above. We also incorporate valence and conduction bands on an equal footing while Yildirim *et al.*[10] included only valence bands. Because this method is non-perturbative, it allows us to study both the metallic and impurity-band regimes, as well as small and large

couplings. Since the strength of the coupling between the magnetic ions and the charge carriers is comparable to the Fermi energy, temporal fluctuations included in our DMFA approach are required in a realistic calculation especially in the vicinity of the critical temperature.

We choose tight-binding parameters according to Chadi and Cohen[11,12], which give the correct band features within a sufficiently wide window of $\pm$ 2.0 eV around the Fermi energy, such as effective masses for valence and conduction bands and the gap at the center of the Brillouin zone. Our model also includes the spin-orbit interaction of the parent material which was proved very important in previous studies of $Ga_{1-x}Mn_xAs$.[13–16] The inclusion of the realistic band structure of the parent material leads to more realistic results. For example, the band repulsion between the conduction band and the impurity band, which was absent in some previous calculations based on the $k \cdot p$ approach[15–18], results in a significant reduction of the bandwidth of the impurity band. Narrowing of the impurity bandwidth increases the localization of the mediating holes, which suppresses the estimated critical temperature. Consequently, we find that the calculated T_c is significantly smaller, and closer to the experimental results.

Model- We model the magnetic interactions in $Ga_{1-x}Mn_xAs$ using the simplified Hamiltonian proposed by Zaránd and Jankó:[13]

$$H = H_0 + J_c \sum_i \mathbf{S}(R_i) \cdot \mathbf{J}(R_i), \qquad (1)$$

where H_0 is a 16×16 matrix including both electronic dispersion and spin-orbit coupling of the sp^3 holes of the parent material. Our tight-binding parameters reproduce the correct band structure for the heavy and light bands around the center of the Brillouin zone, the split-off energy gap and the gap between the valence and the conduction bands[11,12]. The spin-orbit coupling is modeled with a term $\lambda_\alpha \mathbf{L} \cdot \mathbf{S}$ where λ_{Ga} and λ_{As} are interaction constants for Ga and As atoms respectively. The second term in Eq. (1) describes the interaction between Mn
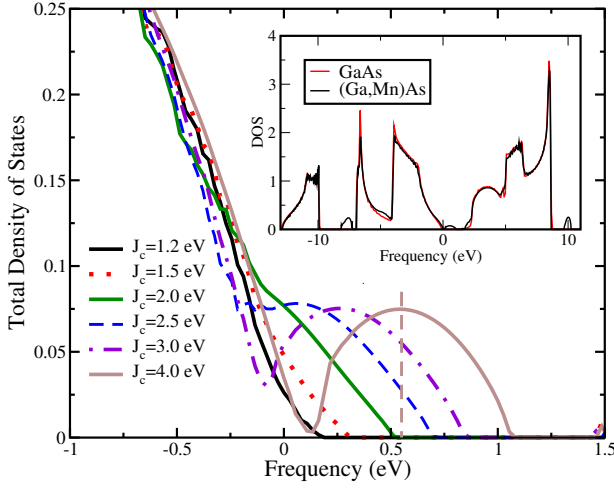
FIG. 1: (color online). Total density of states versus energy at the edge of the valence band for $x = 0.05$, $n_h = x/2 = 0.025$ and several coupling strengths at $T=58$ K. The edge of the conduction band lies at the right bottom corner. The impurity band is not well separated from the valence band up to large couplings ($J_c \sim 4$ eV). The vertical dashed line shows the location of the chemical potential for $J_c=4.0$ eV. Band repulsion between the conduction and impurity bands leads to reduction of the impurity bandwidth. Inset: sp^3 total density of states for pure GaAs and $Ga_{0.95}Mn_{0.05}As$ with $J_c=4.0$ eV. We use a Fourier transform filter to reduce the noise in the calculated density of states. The noise is in regions away from the Fermi energy and is due to the effect of the $\mathbf{k}$ mesh in the coarse graining step of the DMFA self-consistency loop. We have used up to 62,000 $\mathbf{k}$ points in this calculation.

spins and mediating holes, where J_c is the exchange coupling between the localized moments with spin $\mathbf{S}(R_i)$ and the holes total angular momentum density $\mathbf{J}(R_i)$, both at site R_i. Since the spins of Mn^{+2}'s are relatively large ($S = 5/2$) we treat them as classical vectors.

We employ the DMFA algorithm[19] to calculate the magnetic and transport properties of the material within a Green's function formalism[17,18]. We calculate the average magnetization of the manganese ions:

$$M = \frac{1}{\mathcal{Z}} \int d\Omega_s S^z \exp\{-S_{\text{eff}}(\mathbf{S})\} \qquad (2)$$

with the partition function $\mathcal{Z} = \int d\Omega_s \exp[-S_{\text{eff}}(\mathbf{S})]$, and the effective action $S_{\text{eff}}(\mathbf{S}) = -\sum_n \log \det[\hat{\mathcal{G}}_0^{-1}(i\omega_n) + J_c \mathbf{S} \cdot \hat{\mathbf{J}}]$,[20,21] where $\hat{\mathcal{G}}_0$ is the cluster excluded Green function.

The average polarization of the charge carriers at the chemical potential is defined as:

$$\mathcal{P} = \frac{\sum_i j_i^z n_i(\mu)}{\sum_i n_i(\mu)} \qquad (3)$$

where j_i^z is the z component of the total angular momentum and n_i, the density of holes in the ith band.

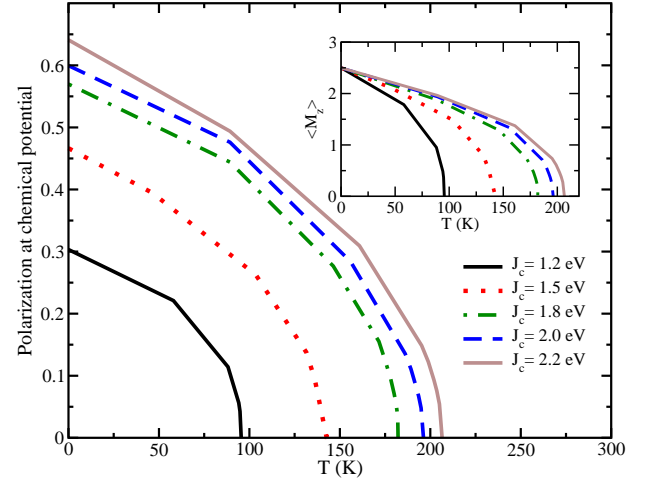To compute the optical conductivity we use the Kubo formula:[22]

FIG. 2: (color online). Average hole polarization versus temperature for different values of J_c at $n_h = x/2 = 0.025$. The polarization is frustrated since it does not reach its maximum allowed value, $\mathcal{P} = 3/2$, at $T = 0$. Comparison with Figure 1 shows that noticeable changes in T_c happens when the impurity band is forming. Inset: Average magnetization of the ions versus temperature for the same couplings.

$$\sigma_{ij}(\omega) = \frac{\pi}{\omega} \int d\nu [f(\nu) - f(\nu + \omega)] \times$$
$$\sum_{\mathbf{k}} Tr[v_i(\mathbf{k})A(\mathbf{k}, \nu + \omega)v_j(\mathbf{k})A(\mathbf{k}, \nu)], \qquad (4)$$

where Tr is the trace, $v_i(\mathbf{k})$ is the velocity along the i direction, $A(\mathbf{k}, \omega)$, the spectral function at momentum $\mathbf{k}$ and frequency ω, and $f(\omega)$, the Fermi function. The group velocities involve the hopping terms in the Hamiltonian and are calculated as $v_i(\mathbf{k}) = \frac{\delta H(\mathbf{k})}{\delta A_i}|_{A=0}$, where H is the Hamiltonian and $\mathbf{A}$ the vector potential.

Results and Discussion- We first focus on the density of states (DOS) of the charge carriers at the doping $x=0.05$ where T_c is among the highest reported.[1,23,24] In Figure 1 and 2 we assume 50% hole compensation due to anti-site and interstitial doping, such that $n_h = x/2 = 0.025$. This corresponds to the optimum filling in the impurity band regime. In any case, the profile of the DOS changes minimally with filling. Figure 1 shows the total density of states at the edge of the valence band for several values of the coupling. Most experimental probes, such as photoemission[25], infrared[26–28] and resonant tunneling[29] spectroscopies, and magneto-transport experiments[30] infer a value of J_c between 0.6-1.5 eV. Within this range of couplings the effect of the magnetic interactions is just a distortion at the edge of the valence band. We have to use coupling strengths as large as 2.5 eV to observe the formation of the impurity band. However, recent scanning tunneling microscopy experiments[31] display an impurity band similar to the one appearing in our results for couplings around $J_c \sim 3.0$ eV.
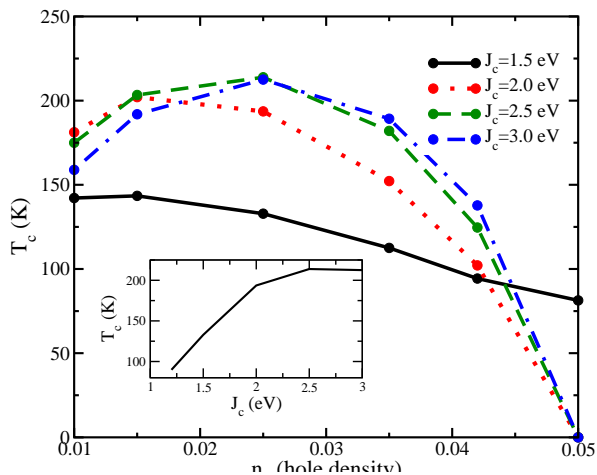
FIG. 3: (color online). T_c versus filling at constant doping, $x=5\%$, for different couplings. For small couplings T_c decreases by increasing the hole concentration. For larger couplings there is an optimum filling of $n_h=2.5\%$ where T_c is maximum. For coupling values lager than 2 eV, T_c does not change appreciably. The inset shows T_c vs. coupling strength for $n_h = x/2$. The saturation of T_c is due to the lack of non-local correlations in the DMFA.
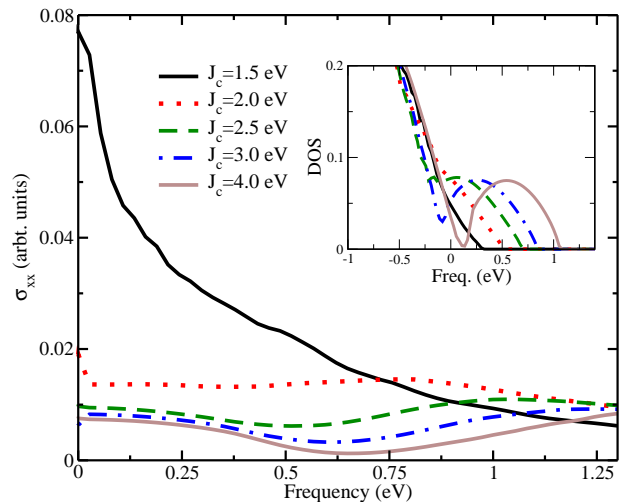

FIG. 4: (color online). Optical conductivity in the direction perpendicular to the magnetization for different couplings at $x=5\%$, $n_h=2.5\%$ and $T=58$ K. The conductivity is suppressed by increasing of J_c due to the increasing localization of the holes. The inset displays the total density of states versus energy at the edge of the valence band for the same parameters.

The impurity band is not completely separated until couplings around ~ 4 eV. As we expected, the repulsion between the conduction and the impurity band confines the latter within the band gap and narrows down the impurity bandwidth. This leads to localization of the charge carriers which in return reduces the ferromagnetic transition temperature, T_c.

Figure 2 displays the temperature dependence of the hole polarization for different couplings. We choose a narrow energy window (~ 0.1 eV) at the chemical potential and calculate the average $\mathcal{P}$ within this window using Eq. (3). The polarization is frustrated since it does not reach its maximum allowed value, $\mathcal{P} = 3/2$, at $T = 0$, and it is further reduced with decreasing magnetic coupling strength. Comparison with Figure 1 shows that noticeable changes in T_c correspond to couplings where the impurity band is forming and separating from the valence band. On the other hand, T_c does not change once the impurity band is fully separated from the valence band. The maximum T_c we obtained is ~ 220 K which is closer to experimental results[32] than previous estimates using the $k \cdot p$ model.[17,18] One can also see the same behavior from the inset which shows the average magnetization of the Mn^{+2} ions versus temperature. However, note that within the DMFA the average magnetization is not frustrated. This is an artifact of DMFA. Inclusion of non-local correlations using cluster methods reduces the value of the magnetization.[15]

Figure 3 displays T_c versus hole filling for $x=5\%$ and different couplings. For large J_c, in the impurity-band regime, T_c is maximum at the optimum filling of $n_h = x/2$. This is consistent with studies based on the impurity band picture.[14,17] For moderate couplings around

$J_c \sim 1.5$ eV and fillings $n_h > 2\%$, T_c increases by decreasing the hole concentration. Recent studies in thin films find T_c to be proportional to the hole concentration for a wide range of n_h values.[33–35] This might indicate a filling larger than the doping, $n_h > x$, in those experiments. The inset in Figure 3 shows T_c versus J_c for fixed hole concentration $n_h = x/2 = 2.5\%$. The plateau at large couplings is due to the absence of non-local correlations within the DMFA.

Finally, we calculate the optical conductivity in the direction perpendicular to the magnetization, σ_{xx}, for energies smaller than the band gap and different couplings (Fig. 4). For small couplings, the conductivity displays a Drude like peak which is suppressed by increasing the coupling. This suppression is due to the increasing bounding between the magnetic ions and the itinerant holes. Our results are in agreement with other theoretical calculations.[9] However, we do not capture the low energy (~ 0.2 eV) peak observed in measurements of the conductivity.[36] The origin of this peak is still highly controversial. While Burch *et al.* explain it as evidence of the existence of the impurity band[36], others explain the result within the distorted valence band picture.[34] Since our results for the density of states do not show any low energy feature for $J_c \leq 2.0$ eV, we do not expect to see any peak in optical conductivity for $J_c \leq 2.0$ eV. Moreover, for large couplings the wide impurity band will induce a feature with similar width. The inclusion of non-local correlations reduces the bandwidth of the impurity band and, it might be possible to capture this low energy peak within a dynamical cluster study.[15]

Conclusions- We study the magnetic and transport properties of the diluted magnetic semiconductor

$Ga_{1-x}Mn_xAs$ within the framework of the multi-orbital DMFA. We employ a semi-empirical sp^3 tight-binding approximation to model the band structure of the parent material. We choose tight-binding parameters according to Chadi,[12] which reproduce the correct band structure within the relevant energy window, including the valence, split-off and conduction bands. The spin-orbit coupling is modeled with a term $\lambda_\alpha \mathbf{L} \cdot \mathbf{S}$. We find that this more realistic band structure leads to more realistic results.

The density of state shows a distorted valence band for moderate coupling strengths, $J_c \sim 1.5$ eV, and an impurity band for couplings larger than $J_c \sim 3.0$ eV. The band repulsion between the impurity and conduction bands reduces the bandwidth of the impurity band. This in turn leads to localization of the itinerant holes and reduction of T_c. The average hole polarization displays a clear magnetic frustration. Moreover, the optical conductivity σ_{xx} shows a Drude-like peak at low frequencies which disappears with increasing couplings. While our conductivity results are similar to previous tight-binding calculations,[9] they do not display the low energy peak observed experimentally.[36] Despite the inclusion of band repulsion effects and that our impurity band is narrower than found previously, it is still too wide. This wide impurity band smears out any low energy features. We believe that the inclusion of corrections including cavity field and non-local correlations into the dynamical mean-field approximation will result in further suppression of the impurity bandwidth and, possibly, development of the peak in the conductivity.

[1] H. Ohno, Science **281**, 951 (1998).

[2] F. Matsukura, H. Ohno, A. Shen, and Y. Sugawara, Phys. Rev. B **57**, R2037 (1998).

[3] T. Dietl, H. Ohno, F. Matsukura, J. Cibert, and D. Ferrand, Science **287**, 1019 (2000).

[4] T. Jungwirth, J. Sinova, J. Mašek, J. Kučera, and A. H. MacDonald, Rev. Mod. Phys. **78**, 809 (2006).

[5] J.-M. Tang and M. E. Flatté, Phys. Rev. Lett. **92**, 047201 (2004).

[6] J.-M. Tang and M. E. Flatté, Phys. Rev. Lett. **101**, 157203 (2008).

[7] J. Mašek, J. Kudrnovský, F. Máca, J. Sinova, A. H. MacDonald, and R. P. Campion, Phys. Rev. B **75**, 045202/1 (2007).

[8] M. Turek, J. Siewert, and J. Fabian, Phys. Rev. B **78**, 085211 (2008).

[9] M. Turek, J. Siewert, and J. Fabian, Phys. Rev. B **80**, R161201 (2009).

[10] Y. Yildirim, G. Alvarez, A. Moreo, and E. Dagotto, Phys. Rev. Lett. **99**, 057207 (2007).

[11] D. J. Chadi and M. L. Cohen, Phys. Stat Sol. (b) **68**, 405 (1975).

[12] D. J. Chadi, Phys. Rev. **16**, 790/1 (1977).

[13] G. Zárand and B. Jankó, Phys. Rev. Lett. **89**, 047201/1 (2002).

[14] J. Moreno, R. S. Fishman, and M. Jarrell, Phys. Rev. Lett. **96**, 237204/1 (2006).

[15] U. Yu, A.-M. Nili, K. Mikelsons, B. Moritz, J. Moreno, and M. Jarrell, Phys. Rev. Lett. **104**, 037201 (2010).

[16] A.-M. Nili, M. A. Majidi, P. Reis, J. Moreno, and M. Jarrell (2010), arXiv:1006.0998.

[17] K. Aryanpour, J. Moreno, M. Jarrell, and R. Fishman, Phys. Rev. B **72**, 045343/1 (2005).

[18] M. Majidi, J. Moreno, M. Jarrell, R. Fishman, and K. Aryanpour, Phys. Rev. B. **74**, 115205/1 (2006).

[19] For a review, see A. Georges, G. Kotliar, W. Krauth, and M. Rozenberg, Rev. Mod. Phys. **68**, 13 (1996).

[20] N. Furukawa, cond-mat/9812066 pp. 1–35 (1998).

[21] N. Furukawa, J. Phys. Soc. Jpn. **63**, 3214/1 (1994).

[22] R. Kubo, J. Phys. Soc. Jpn. **12**, 570 (1957).

[23] D. Chiba, K. Takamura, F. Matsukura, and H. Ohno, Appl. Phys. Lett. **82**, 3020 (2003).

[24] H. Munekata, H. Ohno, S. von Molnar, A. Segmüller, L. L. Chang, and L. Esaki, Phys. Rev. Lett. **63**, 1849 (1989).

[25] J. Okabayashi, A. Kimura, O. Rader, T. Mizokawa, A. Fujimori, T. Hayashi, and M. Tanaka, Phys. Rev. B **58**, R4211 (1998).

[26] M. Linnarsson, E. Janzén, B. Monemar, M. Kleverman, and A. Thilderkvist, Phys. Rev. B **55**, 6938 (1997).

[27] A. K. Bhattacharjee and C. B. á la Guillaume, Sol. St. Commun. **113**, 17 (1999).

[28] E. J. Singley, K. S. Burch, R. Kawakami, J. Stephens, D. D. Awschalom, and D. N. Basov, Phys. Rev. B **68**, 165204/1 (2003).

[29] H. Ohno, N. Akiba, F. Matsukura, A. Shen, K. Ohtani, and Y. Ohno, Appl. Phys. Lett. **73**, 363 (1998).

[30] T. Omiya, F. Matsukura, T. Dietl, Y. Ohno, T. Sakon, M. Motokawa, and H. Ohno, Physica E **7**, 976 (2000).

[31] A. Richardella, P. Roushan, S. Mack, B. Zhou, D. Huse, D. Awschalom, and A. Yazdani, Science **327**, 665 (2010).

[32] K. Y. Wang, K. W. Edmonds, R. P. Campion, B. L. Gallagher, N. R. S. Farley, C. T. Foxon, M. Sawicki, P. Boguslawski, and T. Dietl, J. Appl. Phys **95**, 6512 (2004).

[33] M. Sawicki, D. Chiba, A. Korbecka, Y. Nishitani, J. Majewski, F. Matsukara, T. Dielt, and H. Ohno, Nature Physics **6**, 22/1 (2010).

[34] G. Acbas, M.-H. Kim, M. Cukr, V. Novak, M. A. Scarpulla, O. D. Dubon, and T. Jungwirth, Phys. Rev. Lett. **103**, 137201/1 (2009).

[35] Y. Nishitani, D. Chiba, M. Endo, M. Sawicki, F. Matsukara, T. Dietl, and H.Ohno, Phys. Rev. B **81**, 045208/1 (2010).

[36] K. S. Burch, D. B. Shrekenhamer, E. J. Singley, J. Stephens, B. L. Sheu, R. K. Kawakami, P. Schiffer, N. S. D. D. Awschalom, and D. N. Basov, Phys. Rev. Lett. **97**, 087208/1 (2006).